Transactions, SMiRT-26
Berlin/Potsdam, Germany, July 10-15, 2022
Division V

EXTENDED NUREG-BASED METHOD FOR DUCTILITY COEFFICIENT ASSESSMENT OF NPP BUILDINGS

Miquel Huguet[1], Silvano Erlicher[2], Elias Bou-Said[2], Philippe Bisch[2], Etienne Gallitre[3], Alexis Courtois[4]

[1] Civil Engineer, PhD, EGIS, Montreuil (France) (miquel.huguet-aguilera@egis.fr)
[2] Expert, EGIS, Montreuil (France)
[3] Expert, Gallitre Consultant, Verneiges (France)
[4] Expert, EDF, Lyon (France)

ABSTRACT

Reinforced Concrete (RC) structures submitted to relatively high-intensity seismic actions show a mechanical behaviour beyond the linear elastic domain. This phenomenon is at the origin of the ductility (absorbing displacements without major force softening) so of a capacity of energy dissipation that provides a seismic margin to the structure to resist the earthquake. This effect is expressed with the ductility coefficient F_μ that accounts for the reduction of the structural forces calculated with a linear elastic model. This paper assesses the global ductility coefficient F_μ of a NPP building using the approach proposed by Ruocci et al. (2016), which is inspired by the NUREG (1985) guide. The results of a single linear elastic analysis are used to compute the imposed F_μ of each structural element. Then, the ductility of each element is calculated using the "effective frequency / effective damping" approach. This procedure is repeated by increasing the PGA value up to attain the failure of the critical element (which corresponds to the failure of the structure). The proposed approach is applied to a large 3D model of a NPP building, analyzing the effects of taking into account the available mechanical experimental results of some critical elements (see companion paper Huguet et al. 2022), the reduction of the concomitant axial force and the Soil-Structure Interaction (SSI). The obtained results show a relatively ductile behavior of the structure arising to relatively high seismic margin due to the global ductility coefficient F_μ.

INTRODUCTION

Non-linear transient and pushover analyses have been developed in the last decades to calculate a more realistic seismic response than the one obtained using linear elastic assumptions. However, the seismic forces on Nuclear Power Plant (NPP) buildings are still commonly calculated using linear elastic analyses because they are less time-consuming when carried out on large 3D Finite Elements (FE) models of Reinforced Concrete (RC) structures. In this case, as the obtained seismic forces are overestimated and seismic displacements are underestimated when the structural response goes beyond the elastic limit state, the calculation of seismic margins from a linear structural analysis requires the so-called ductility coefficient F_μ to be used. We consider two types of ductility coefficients:

- The *local* ductility coefficient referred to a structural element, as the ones provided by IAEA (2003) and ASCE-SEI (2005) codes. The *companion* paper Huguet et al. (2022) presents the estimation of local F_μ coefficients of two RC walls and one RC slab representative of NPP's RC elements that have been tested in an experimental campaign, using the "effective frequency / effective damping" approach proposed by NUREG (1984) and EPRI (1994).

- The *global* ductility coefficient referred to the overall ductility of the structure. EPRI recommendations [EPR94] are based on the mean ductility referred to the whole structure. NUREG (1984) proposes to evaluate non-linear drifts of the main structural walls for a given response spectrum with a reference Peak Ground Acceleration (PGA), by carrying out a post-treatment of the efforts obtained by a linear elastic analysis.

In this work, we consider the approach proposed by Ruocci et al. (2016), which is inspired by NUREG guide, for the calculation of the global ductility coefficient of a NPP structure. The results of a linear elastic analysis are used to compute the inelastic drift of each structural element. The static linear analysis provides the distribution of the non-seismic efforts D_{ns}. The seismic linear analysis at reference PGA value PGA_{ref} provides the distribution of the reference seismic efforts $D_{s,ref}$. Then, the seismic efforts are increased proportionally to the considered PGA value up to that the *critical element* reaches its failure for the *critical failure mode* for the *critical seismic combination*:

- The *critical element* is the first element that reaches failure
- *Failure* conventionally occurs when the non-linear drift of an element equals its ultimate drift, for at least one of the *failure modes* that can occur in the considered element, and for at least one of the considered seismic combinations. The failure modes for 2D RC elements are associated to the following two efforts D: the global shar force V and the in-plane moment M.

At this instant, this value of PGA defines the ultimate PGA_u, so that the seismic margin F is calculated with respect to the reference PGA value PGA_{ref}:

$$F = \frac{PGA_u}{PGA_{ref}} \tag{1}$$

This seismic margin is commonly expressed as the product of the ductility factor F_μ and the *elastic margin factor* F_{se}, which depends on the possible failure modes:

$$F = F_\mu F_{se} = \tilde{F}_\mu \tilde{F}_{se} \tag{2}$$

Two different definitions of these coefficients can be considered depending whether there are associated calculated with the elastic limit V_y (F_{se}) or the capacity C ($\tilde{F}_{se}$):

- They are calculated with respect to the PGA value PGA_y at which the critical element reaches its elastic resistance V_y (NUREG guide definition):

$$F_\mu = \frac{PGA_u}{PGA_y} \qquad F_{se} = \frac{V_y - D_{ns}}{D_{s,ref}} = \frac{PGA_y}{PGA_{ref}} \tag{3}$$

- They are calculated with respect to the PGA value PGA_c at which the critical element reaches its capacity C (EPRI (1994), ASCE (2005), IAEA (2003) definition):

$$\tilde{F}_\mu = \frac{PGA_u}{PGA_c} \qquad \tilde{F}_{se} = \frac{C - D_{ns}}{D_{s,ref}} = \frac{PGA_c}{PGA_{ref}} \tag{4}$$

Figure 1 shows the graphical interpretation of the notion of ductility coefficient for a Single-Degree-of-Freedom (SDoF) oscillator for both cases.

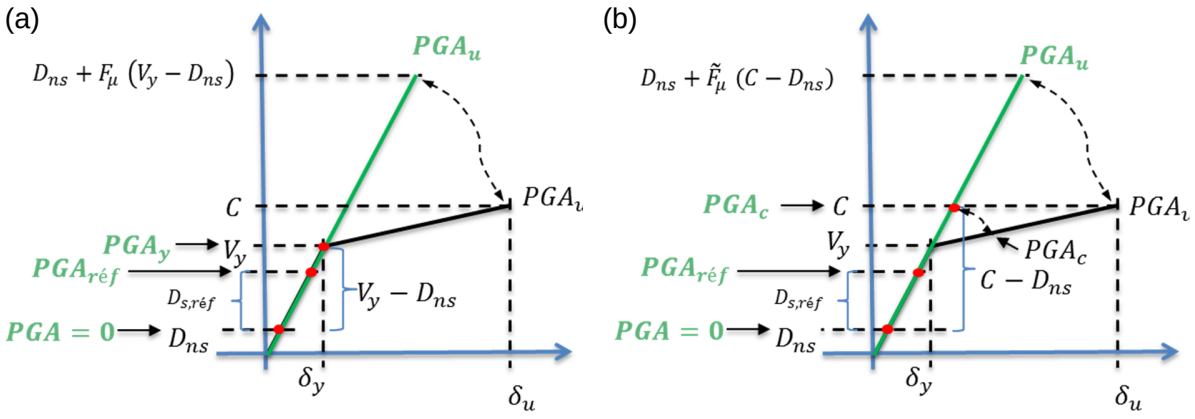

Figure 1. Characterisation of a bilinear force-displacement curve for the calculation of F_μ.

RETAINED APPROACH FOR GLOBAL DUCTILITY COEFFICIENT ASSESSMENT

We recall here the approach proposed by Ruocci et al. (2016) for the calculation of the global ductility coefficient F_μ for a NPP building using the results of a linear elastic seismic structural analysed. It is an extension to a 3D structural model of the NUREG guide approach, which is defined for a stick model. The approach is detailed in the steps listed hereinafter and summarised in Figure 2.

The needed input data are the static and seismic results of a linear elastic calculation performed on a FE model:

1) Create the 3D linear elastic structural model of the building
2) Compute the static calculation with permanent loads and loads concomitants to the earthquake -> D_{ns} non-seismic efforts distribution
3) Compute a response-spectrum analysis for PGA_{ref} and combine the mode and direction combinations (in the example of next chapter, this is done with CQC and Newmark combinations) -> $D_{s,ref}$ seismic efforts distribution at PGA_{ref} for all the elements and seismic combinations
4) (Optional) Identify a certain number of elements with relatively low values of F_{se} in order to limit the calculations in the iterative steps of the procedure
5) Identify the possible failure modes of the considered elements.

Then, <u>for every retained element, seismic combination and failure mode</u>:

6) Calculate the elastic limit V_y and the capacity C, associated to a bilinear behaviour assumption of the considered failure modes. When these limits are expressed in terms of a resistance domain in a plane depending on concomitant efforts (commonly the axial force N), the entire domain has to be calculated. The formulas provided by EPRI (1994) can be retained for 2D RC elements.
7) Calculate the imposed ductility coefficient $F_{\mu,imp}$ defined as the ratio of the seismic demand and the available elastic limit, or the inverse of the elastic seismic margin:

$$1 = F = F_{se}F_\mu \rightarrow F_{\mu,imp} = \frac{1}{F_{se}} = \frac{D_s}{V_y - D_{ns}} \tag{5}$$

Then, for all elements, seismic combinations and failure modes for which the imposed ductility coefficient $F_{\mu,imp}$ is greater than 1:

8) Identify the « dominant » eigenfrequency of the structure creating the main contribution at seismic efforts D_s
9) Create the curve $F_{\mu,1ddl}$ vs. μ with the "effective frequency / effective damping" approach (NUREG (1984) and EPRI (1994)) for the considered seismic response spectrum. The SDoF force-displacement curves are defined by the elastic limit V_y and the capacity C calculated in step 6) and the numerical stiffness of the element in the 3D linear elastic FE model of the building used for the seismic analysis in step 3). Plot two other curves using Table 1 to consider the uncertainties by computing ductility values $\mu_{e,1}$ and $\mu_{e,2}$.

Table 1: Errors on F_μ given by NUREG (1984)

μ	Error on F_μ
2	+/-15%
4	+/-20%
6	+/-25%
8	+/-30%
10	+/-35%

10) Using the curves determined in the step before, find the effective ductility range $\mu_{e,1}$ et $\mu_{e,2}$ which are associated to the uncertainties. This ductility values are obtained with the assumption of a SDOF structural behaviour so an identical yielding of all the structural elements. This assumption underestimates the ductility of the critical elements and overestimates the average ductility of the structure
11) Take into account the structural effect by using the coefficient M_e (which is equal to 1 for SDOF or MDOF regular structures where all the structural elements have an uniform demand/capacity ratio). NUREG (1985) recommends using values between 1,8 and 2,0 for irregular structures. This coefficient has a great importance in this method and could be better assessed from nonlinear structural analyses:

$$\mu_{m,1} = M_e(\mu_{e,1} - 1) + 1 \qquad \mu_{m,2} = M_e(\mu_{e,2} - 1) + 1 \tag{6}$$

12) Compare the obtained ductility values (actually, only the comparison the maximum value $\mu_{m,2}$ is necessary) with the maximum drift δ_u associated to the mode failure:

$$\mu_{m,2}\delta_y \leq \delta_u \leftrightarrow \mu_{m,2} \leq \mu_{m,u} = \frac{\delta_u}{\delta_y} \tag{7}$$

13) When $\mu_{m,2} = \mu_{m,u}$ for at least one element, seismic combination and failure mode, stop the procedure, retain the actual value of PGA as PGA_u and calculate F, F_μ and F_{se} with Equation (1) and Equation (3) or Equation (4)

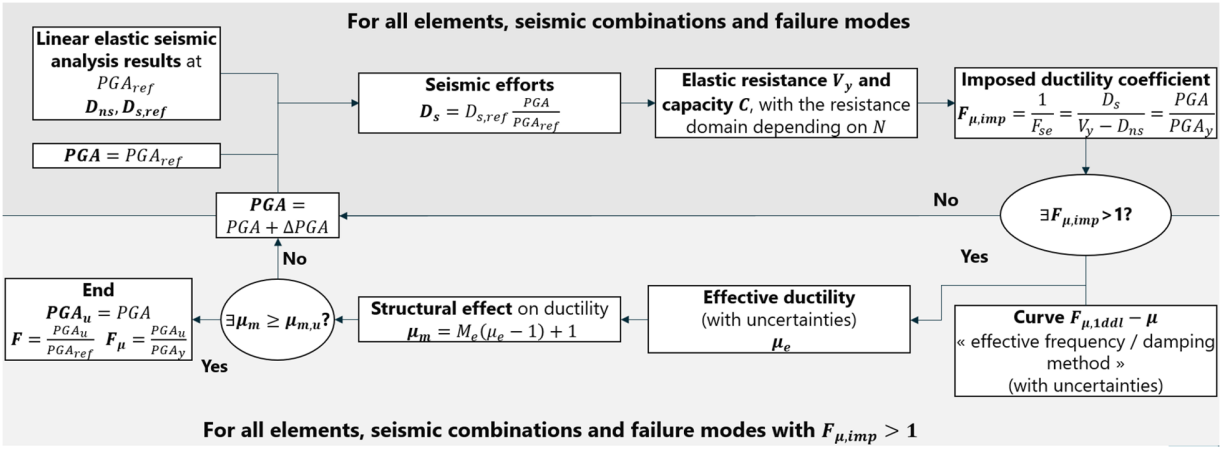

Figure 2. Summary of the proposed procedure for the calculation of F and F_μ.

Accounting for SSI

Ruocci et al. (2016) propose a method to consider Soil-Structure Interaction (SSI) with a simplified approach considering that the soil-structure system acts as an oscillator with one mass and two springs in series: the soil-foundation interface spring in series with the RC structure spring. This scheme makes possible to distinguish the loss of stiffness due to RC cracking and plasticity, which concerns only the RC structure, from the loss of stiffness due to the soil-foundation uplift, to be associated with the soil spring only (in this paper, no soil-foundation uplift is considered). Based on the "effective frequency / effective damping" approach (NUREG (1984) and EPRI (1994)), which accounts for a secant frequency f_s calculated from the elastic frequency f using the ratio between the secant ($k_{RC,s}$) and the elastic RC stiffness (k_{RC}), Ruocci et al. (2016) propose to calculate the secant stiffness with:

$$\left(\frac{f_s}{f}\right)^2 = \frac{k_{RC,s}}{k_{RC}}\frac{k_{soil}+k_{RC}}{k_{soil}+k_{RC,s}} = \frac{k_{RC,s}}{k_{RC}}\frac{1+\frac{k_{soil}}{k_{RC}}}{\frac{k_{soil}}{k_{RC}}+\frac{k_{RC,s}}{k_{RC}}} \tag{8}$$

where the ratio between the soil and RC structure stiffness is calculated using the main modal frequency and mass for the case of rigid structure and elastic soil (f_{soil},M_{soil}) and for the case of rigid soil and elastic structure (f_{RC},M_{RC}):

$$\frac{k_{soil}}{k_{RC}} = \frac{f_{soil}^2 M_{soil}}{f_{RC}^2 M_{RC}} \tag{9}$$

The other steps of the "effective frequency / effective damping" approach are not modified.

APPLICATION TO A NPP BUILDING

Considered NPP building

We consider the NPP building presented in Figure 3. We consider the 24 Newmark seismic combinations obtained with a linear elastic response-spectrum analysis, considering the seismic spectrum of Figure 4. An elastic seismic analysis has shown that only a small number of RC elements are critical, see the elements highlighted in Figure 3, when considering the following failure modes assessed with EPRI (1994) capacity formulas:

- In-plane flexion, associated to an ultimate drift of $\delta_u = 0{,}7\%$

- In-plane diagonal shear cracking, associated to an ultimate drift of $\delta_u = 0{,}5\%$
- Shear friction

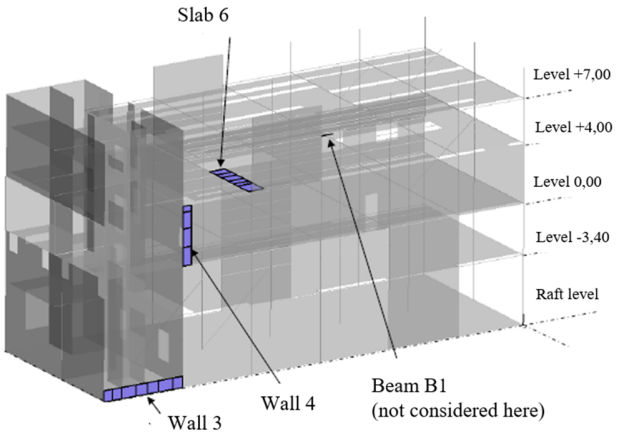

Figure 3. Considered NPP structure and critical elements

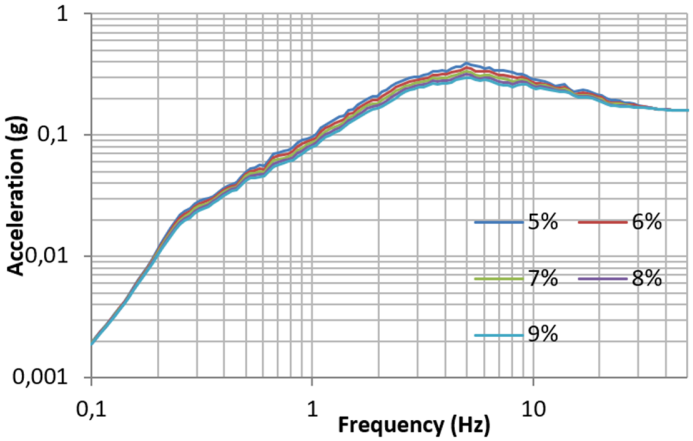

Figure 4. Seismic response spectrum

Considered critical elements and associated experimental results

For simplicity, here we consider only these three elements in the calculation of the global ductility coefficient F_μ using the approach described in the previous chapter: RC walls 3 and 4 and RC slab 6. Moreover, 8 mock-ups representing these 3 RC elements have been tested experimentally, see the *companion* paper Huguet et al. (2022). The available experimental results are global shear force V vs. horizontal displacement δ curves of the three critical elements of the structure for which some results in terms of stiffness, capacity and ductility can be used. However, these results are only valid for the combination used in the test for the applied global shear force V and concomitant axial force N. Since the calculation of F_μ has to be performed for all the 24 seismic Newmark combinations, the experimental results cannot be used in a general case. It has been decided to use the experimental results to apply a correction of the theoretical bending moment – axial force resistance domain given by EPRI (1994), since this one is the failure mode observed experimentally in the tests. The last line of Table 2 gives the coefficient that it is

applied to the EPRI resistance domain. The calculations of F_μ are performed with the two resistance domains.

Table 2: Average experimental/EPRI ratio for capacity of RC walls 3 and 4 and RC slab 6

Element	RC Wall 3		RC Wall 4			RC Slab 6
Test n° (Huguet et al. 2022)	3	4	5	8-pos	8-neg	6
C experimental	1,95MNm	2,13MNm	4,76MNm	4,06MNm	3,33MNm	2,04MNm
C EPRI (1994)	0,47MNm	1,09MNm	3,14MNm	3,81MNm	3,81MNm	2,74MNm
Ratio exp/EPRI	4,1	1,9	1,5	1,1	0,9	0,7
Average ratio exp/EPRI	3,0		1,2			0,7

Obtained results

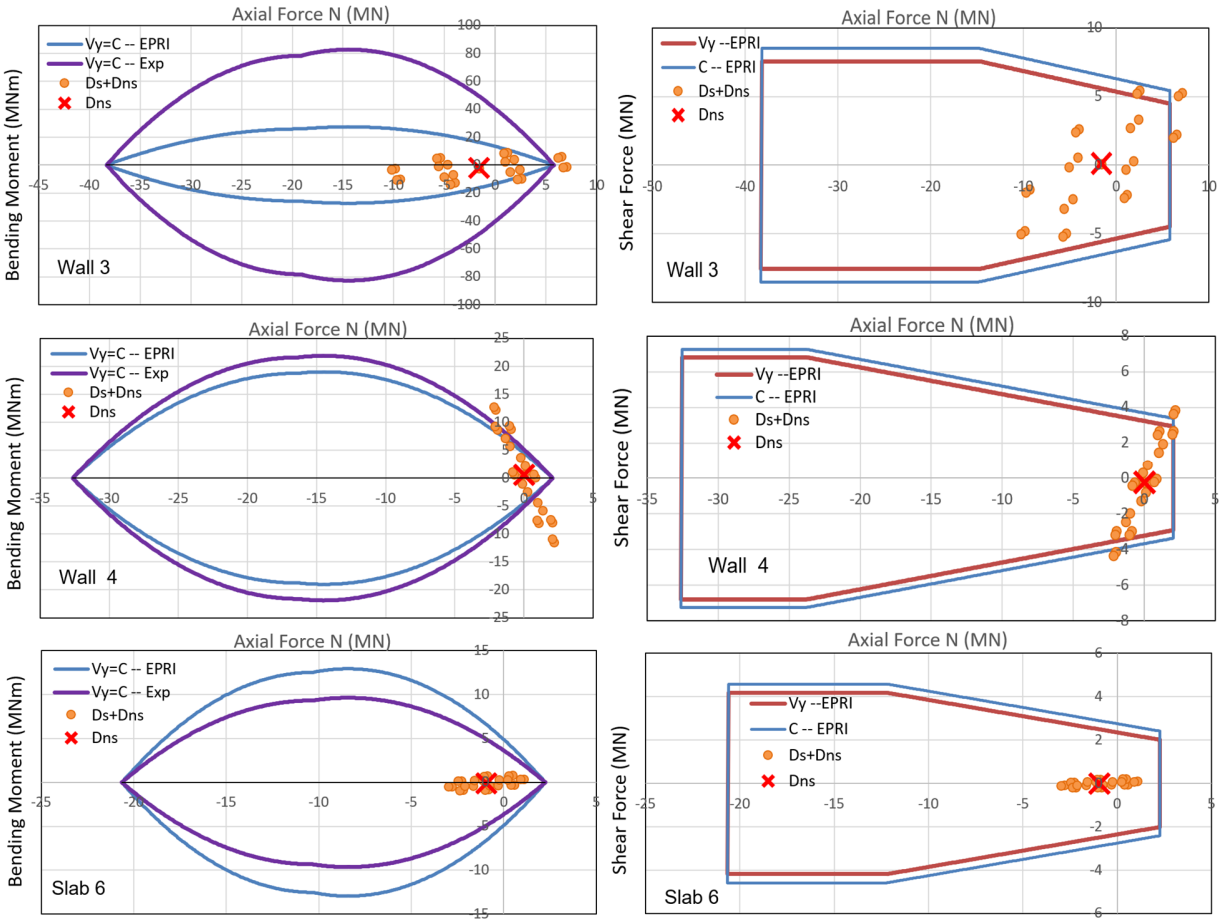

Figure 5. Resistance domains (in-plane bending moment and shear) for RC walls 3 and 4 and RC slab 6 at $PGA = PGA_{ref} = 0{,}3g$

The first iteration at $PGA_{ref} = 0{,}3g$ shows that RC walls 3 and 4 need $F_{\mu,imp} > 1$ for some seismic combinations which are outside the resistance domain (elastic margin factor $F_{se} \leq 1$), see Figure 5. The

shear fraction failure mode is never reached so, for simplicity, it is neglected in the following figures and tables. Also, the seismic combinations that reach the diagonal shear cracking resistance domain in the axial force zone are treated as (i) a particular case of the in-plane flexion ductile failure mode in the following calculations and (ii) as a non-ductile failure mode in the sensibility analysis at the end of this section.

The steps 8-13 of the retained approach are performed for each seismic combination with $F_{\mu,imp} > 1$ for RC walls 3 and 4, showing that the imposed ductility coefficient can be absorbed by the ductility of these elements. The associated structural frequencies creating the main efforts in the elements (and used in the "effective frequency/effective damping" approach) are 3,46Hz for RC walls 3 and 4 and RC slab 6. The value of the PGA is increased up to reaching the ultimate ductility for the critical element for the critical failure mode and for the critical seismic combination. This is obtained for $PGA_u = 0{,}802g$ for which RC wall 4 attains the ultimate drift $\delta_u = 0{,}7\%$ for the diagonal shear cracking for Newmark seismic combination 8. At this PGA level, the comparison between elastic efforts and resistance domain is presented in Figure 6 for the three considered elements.

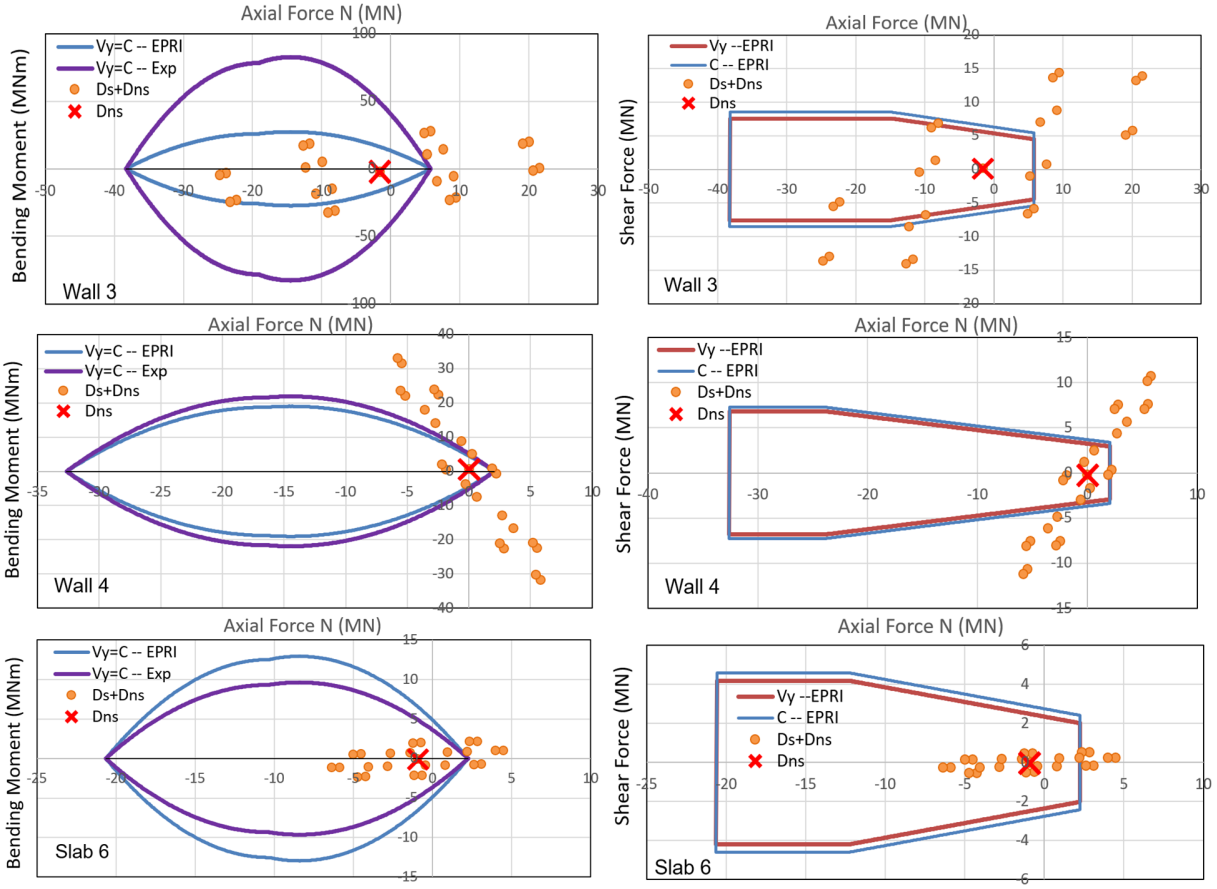

Figure 6. Resistance domains (in-plane bending moment and shear) for RC walls 3 and 4 and RC slab 6 at $PGA = PGA_u = 0{,}802g$

Table 3: Critical seismic combinations of RC walls 3 and 4 and RC slab 6 at $PGA_u = 0{,}802g$

RC element	Failure mode	Critical Newmark seismic combination	$F_{\mu,imp}$	μ	$\mu_{e,2}$	$\mu_{m,2}$	$\mu_{m,u} = \frac{\delta_u}{\delta_y}$	$\frac{\mu_{m,2}}{\mu_{m,u}}$
RC wall 3	In-plane flexion (EPRI)	11	3,68	12,0	24,4	45,4	421,3	0,108
	In-plane flexion (exp.)	11	3,21	8,9	17,8	32,9	339,8	0,097
	Diagonal shear cracking	1	2,91	5,3	10,5	19,0	58,8	0,322
RC wall 4	In-plane flexion (EPRI)	1	9,11	37,4	83,6	157,9	172,1	0,917
	In-plane flexion (exp.)	1	8,53	34,3	73,3	138,3	159,2	0,868
	Diagonal shear cracking	8	3,40	6,7	13,0	23,9	23,9	1
RC slab 6	In-plane flexion (EPRI)	15	1,47	1,6	1,8	2,6	330,8	0,008
	In-plane flexion (exp.)	15	1,57	1,7	2,0	3,0	354,6	0,008
	Diagonal shear cracking	-	-	-	-	-	-	-

The results are summarised in Table 3 for the critical Newmark seismic combination for each considered failure mode for each considered RC element at $PGA_u = 0{,}802g$. The critical element is RC wall 4 for the critical failure mode diagonal shear cracking (even if we note that in-plane flexion is also associated to $\mu_{m,2}/\mu_{m,u}$ values near to 1). It is observed that the experimental results used in the calculations have no effect on the determination of PGA_u because they only affect the resistance of the in-plane flexion fracture mode which is not the failure mode. RC wall 3 and RC slab 6 show that they still have ductility margin (small values of $\mu_{m,2}/\mu_{m,u}$) at $PGA_u = 0{,}802g$. Therefore, the global seismic margin F, the ductility coefficient F_μ and the elastic margin factor F_{se} are given by Newmark seismic combination 8 for diagonal shear cracking failure mode for RC wall 4:

$$F = \frac{PGA_u}{PGA_{ref}} = \frac{0{,}802g}{0{,}3g} = 2{,}67 \qquad F_\mu = \frac{PGA_u}{PGA_y} = \frac{0{,}802g}{0{,}236g} = 3{,}40 \quad F_{se} = \frac{PGA_y}{PGA_{ref}} = \frac{0{,}236g}{0{,}3g} = 0{,}79 \quad (10)$$

When ISS is considered in the "effective frequency/effective damping" approach using Equation (8) with the ratio $k_{soil}/k_{RC} = 6{,}7$ calculated using Equation (9) (with $f_{soil} = 9{,}33Hz$, $M_{soil} = 5010tons$, $f_{RC} = 4{,}25Hz$, $M_{RC} = 3600tons$), there is an impact in the obtained F_μ vs. μ relationship, which is used for estimating μ (and so $\mu_{e,2}$ and $\mu_{m,2}$) from $F_{\mu,imp}$. The obtained values of ductility are slightly lower so the comparison with $\mu_{m,u}$ is also slightly lower. Therefore, the obtained $PGA_u = 0{,}841g$ is higher than in the reference case and the values of F and F_μ are also higher (elastic margin factor F_{se} does not depend on the ductility so it remains constant):

$$F = \frac{PGA_u}{PGA_{ref}} = \frac{0{,}841g}{0{,}3g} = 2{,}80 \qquad F_\mu = \frac{PGA_u}{PGA_y} = \frac{0{,}841g}{0{,}236g} = 3{,}56 \quad F_{se} = \frac{PGA_y}{PGA_{ref}} = \frac{0{,}236g}{0{,}3g} = 0{,}79 \quad (11)$$

Finally, it is noted that if we consider that tensile force failure mode is not ductile (and cannot be treated as a particular case of in-plane flexion as it has been done in this paper), the seismic efforts which are outside the resistance domain in the tensile are in Figure 5 cannot be justified since $F_{se} < 1$ and $F_\mu = 1$ (no ductility), so $F < 1$. In this case, the seismic margin is obtained by reducing the PGA value from PGA_{ref} to $PGA_u = 0{,}234g$ using EPRI resistance domain and $PGA_u = 0{,}248g$ using the resistance

domain corrected with the experimental results. For the example of EPRI resistance domain, the global seismic margin F, the ductility coefficient F_μ and the elastic margin factor F_{se} read):

$$F = \frac{PGA_u}{PGA_{ref}} = \frac{0{,}234g}{0{,}3g} = 0{,}78 \qquad F_\mu = \frac{PGA_u}{PGA_y} = \frac{0{,}234g}{0{,}234g} = 1 \quad F_{se} = \frac{PGA_y}{PGA_{ref}} = \frac{0{,}234g}{0{,}3g} = 0{,}78 \qquad (12)$$

CONCLUSION

This paper calculates the global ductility coefficient F_μ (and the seismic margin F) for a NPP building structure accounting for its ductile behaviour. Using the extended NUREG-based method of Ruocci et al. (2016), the results of a linear elastic structural analysis are treated using the "effective frequency/effective damping" approach for each critical element of the structure. The obtained results show a relatively ductile behaviour of the structure arising to relatively high global seismic margin F (calculated with respect to $PGA_{ref} = 0{,}3g$) due to the global ductility coefficient F_μ, which compensates low values of elastic margin factor $F_{se} < 1$. For the seismic behaviour of the structure, when ISS is taken into account in the "effective frequency/effective damping" approach the obtained global seismic margin and ductility coefficients are slightly higher. Finally, it is remarked that these results are obtained by considering tensile force as a particular case of in-plane moment; if the ductility of tensile failure is neglected, the obtained global seismic margin and ductility coefficients are drastically reduced.

REFERENCES

ASCE/SEI, 43-05, Seismic Design Criteria for Structures, Systems and Components in Nuclear Facilities, 2005

EPRI (1994), TR-103959 Research Project – *Methodology for Developing Seismic Fragilities*.

Huguet, M., Bisch, P., Bou-Said, E., Gallitre, E., Mertz, P.Y., Merle, P., Meuzard, R. (2022). "Ductility coefficient assessment for RC walls and slabs submitted to experimental tests", *Proc., SMiRT 26*, IASMiRT, Berlin

IAEA (2003). *Safety Reports Series No.28 – Seismic Evaluation of Existing Nuclear Power Plants*

NUREG (1984). CR-3805 – *Engineering Characterization Of Ground Motion – Task II Vol.2 - Effects of Ground Motion Characteristics on Structural Response Considering Localized Structural Nonlinearities and Soil-Structure interaction Effects*.

Ruocci, G., Erlicher, S., Bou-Said, E., Do, T.L., Gallitre, E. (2016). "Application of an extended NUREG-based method to estimate the ductility coefficient of a NPP building", *Proc., Technological Innovations in Nuclear Civil Engineering*, SFEN, Paris, France.